


Compared Two Models for Shifted the Gap Energy in Acenes; Quantum Perturbation Theory and Topological Indices

Bahare Agahi Keshe¹ and Ali Iranmanesh^{2*} 

¹Department of Mathematics, Science and Research Branch, Islamic Azad University, Tehran, Iran

²Department of Mathematics, Faculty of Mathematical Sciences, Tarbiat Modares University, Tehran, Iran

Keywords:

Acenes,
Spin-orbit effect,
Gap energy changes,
Nanostructure,
Topological indices

AMS Subject Classification (2020):

05C09; 05C92; 05C07

Article History:

Received: 2 January 2024

Accepted: 29 March 2024

Abstract

Acenes, which can be represented by the chemical formula $C_{4n+2}H_{2n+4}$, belong to a group of organic molecules that have attracted significant attention in the fields of electronic molecules and nanoscale research. Investigating their electronic and optical properties, particularly for larger acenes, is a highly resource-intensive and time-consuming endeavor. The objective of this study is to propose a novel approach for analyzing changes in the energy gap using quantum perturbation theory and disorder theory, relying on topological indices. In order to quantify the alterations in the energy gap, the Hamiltonian matrix of spin-orbit interaction, based on quantum perturbation theory, has been utilized. Consequently, the changes in the energy gap between singlet and triplet states, denoted as E_g , have been computationally determined for the carbon-carbon bonds. Ultimately, a comprehensive model has been developed to illustrate the variations in the energy gap between singlet and triplet spin states of linear acenes, incorporating the concept of topological indices.

© 2024 University of Kashan Press. All rights reserved.

1 Introduction

Molecular electronic, or molectronic, is a branch of nano-electronic that discusses the whatness and use of small groups of molecules on nanoscale or single molecules in electronic circuits. The production of electronic circuits through a single-molecule approach is the ideal perspective of nano-electronic. Therefore, attention to micro-structured pieces in recent years has resulted in the emergence of nano-electronic branches [1, 2]. Acenes, which have a chemical formula

*Corresponding author

E-mail addresses: bahare.agahi@yahoo.com (B. Agahi Keshe), iranmanesh@modares.ac.ir (A. Iranmanesh)

Academic Editor: Gholam Hossein Fath-Tabar

of $C_{4n+2}H_{2n+4}$, are a group of organic molecules that have garnered considerable attention in the fields of electronic molecules and nanoscale. Recent discoveries have revealed that larger acenes, consisting of six to 10 rings, can be found in volcanic ash and interplanetary dust. These larger acenes exhibit remarkable suitability for use in electronic components [3]. However, the exploration and analysis of this family of nano-structures necessitates substantial investments in terms of both time and finances. Therefore, it would be greatly advantageous to have a reliable pattern that can accurately predict the electronic characteristics of acenes. Topological indices offer a cost-effective and practical approach to achieve this objective.

Topological indices have been devised in the field of chemistry to analyze molecular graphs, and they are represented based on graph properties such as connectivity and vertex distances. These indices enable the description and prediction of various chemical, physical, and electronic characteristics of the molecule [4, 5]. They are categorized into distinct branches depending on their specific definitions [6].

In a scholarly article by Ivan Gutman, three noteworthy topological indices were presented. These indices are denoted as RM_2 (reduced second Zagreb index), RR (reduced Randić index), and RRR (reduced reciprocal Randić index) [7].

In this paper, we present a new model based on topological indices for gap energy changes in a linear acene family. Thus, RR , RM_2 , and RRR topological indices will be scrutinized in a linear acene family and the estimated values will be compared with those obtained from the quantum model.

2 Definitions and notations

A graph is a set of points and connecting lines, which are also referred to as vertices and edges, respectively. When an edge, denoted as e , connects two vertices, i and j , it is written as $e = ij$, indicating that i and j are adjacent. A graph is called connected if there exists at least one path between every pair of vertices.

One practical application of graph theory in the field of chemistry involves quantifying chemical structures using graph invariants. These invariants can take the form of polynomials, spectra, atomic properties, or molecular topological indices [8–10].

A topological index is a numerical representation derived from specific topological attributes of a molecular graph, capturing key characteristics of the molecular structure. These indices play a crucial role in quantifying structural similarity or diversity, thereby offering valuable insights into the variety present in chemical databases. The primary objective of employing topological indices is to serve as numerical descriptors for chemical structures within QSPR and QSAR models, facilitating their analysis and prediction ([11–22]). Since isomorphic graphs exhibit identical values for any given topological index, these indices remain unchanged regardless of the labeling of the molecular graph. The topological indices for $RR(G)$, $RRR(G)$, and $RM_2(G)$ are defined as follows [7]:

$$RR = RR(G) = \sum_{ij \in E(G)} \sqrt{d_i d_j}, \quad (1)$$

$$RM_2 = RM_2(G) = \sum_{ij \in E(G)} (d_j - 1)(d_i - 1), \quad (2)$$

$$RRR = RRR(G) = \sum_{ij \in E(G)} \sqrt{(d_j - 1)(d_i - 1)}, \quad (3)$$

where d_i is the degree of vertex i . So the bra-ket notation is the following: Say we have two quantum states ϕ and ψ . Those are vectors in an inner product space. The inner product

between them is $\langle \phi | \psi \rangle$. In a stroke of weird notation, physicists denote the vector ψ by $|\psi\rangle$. This is called a ket, since it is the later part of a bracket. This has the perk that if φ_n is a collection of vectors then we can denote the kets by $|n\rangle$ instead of $|\varphi_n\rangle$.

In the bond between two carbon atoms, electrons are coupled together in the second level ($n = 2, L = 1$) and occupy singlet and triplet states, as shown in the following [23]:

$$|\kappa_{T,1}\rangle = \left| \frac{1}{2}, \frac{1}{2} \right\rangle_1 \left| \frac{1}{2}, \frac{1}{2} \right\rangle_2, \quad (4)$$

$$|\kappa_{T,0}\rangle = \frac{1}{\sqrt{2}} \left(\left| \frac{1}{2}, \frac{1}{2} \right\rangle_1 \left| \frac{1}{2}, -\frac{1}{2} \right\rangle_2 + \left| \frac{1}{2}, -\frac{1}{2} \right\rangle_1 \left| \frac{1}{2}, \frac{1}{2} \right\rangle_2 \right), \quad (5)$$

$$|\kappa_{T,-1}\rangle = \left| \frac{1}{2}, -\frac{1}{2} \right\rangle_1 \left| \frac{1}{2}, -\frac{1}{2} \right\rangle_2, \quad (6)$$

$$|\kappa_{S,0}\rangle = \frac{1}{\sqrt{2}} \left(\left| \frac{1}{2}, \frac{1}{2} \right\rangle_1 \left| \frac{1}{2}, -\frac{1}{2} \right\rangle_2 - \left| \frac{1}{2}, -\frac{1}{2} \right\rangle_1 \left| \frac{1}{2}, \frac{1}{2} \right\rangle_2 \right). \quad (7)$$

Indices 1 and 2 in the above equations are related to the first and second electrons respectively. This interaction yields the following eigenfunctions [23]:

$$|\psi_{T,m_s}\rangle = |\phi(\vec{r})\rangle |\kappa_{T,m_s}\rangle, \quad (8)$$

$$|\psi_{S,0}\rangle = |\phi(\vec{r})\rangle |\kappa_{S,0}\rangle. \quad (9)$$

In the above equations, $|\phi(\vec{r})\rangle$ denotes the spatial part of the wave function. On the other hand, this spin-orbit interaction is presentable through the following Hamiltonian [23, 24]:

$$H_{L-S} = H_{1(L-S)} + H_{2(L-S)} = 2 \left[\frac{1}{2\mu c^2} \frac{1}{r} \frac{dV(r)}{dr} \right] = \frac{1}{\mu c^2} \frac{1}{r} \frac{dV(r)}{dr} \left[\frac{1}{2} (L_+ S_- + L_- S_+) + L_z S_z \right], \quad (10)$$

where μ is reduced electron mass, $V(r)$ is potential energy, \vec{L} and \vec{S} are the extents of spin and orbital angular momentum respectively, and c is the speed of light. Both electrons have similar conditions and, consequently, have similar Hamiltonian. This Hamiltonian results in ground energy change and a fine structure, which is calculated using perturbation theory in quantum mechanics.

3 Methods

3.1 Quantum investigation of gap energy change

To calculate the shift of gap energy, a Hamilton matrix of spin-orbit interaction of Equation (8) has been used:

$$H_{L-S} = \begin{bmatrix} H_{11} & H_{12} & H_{13} & H_{14} \\ H_{21} & H_{22} & H_{23} & H_{24} \\ H_{31} & H_{32} & H_{33} & H_{34} \\ H_{41} & H_{42} & H_{43} & H_{44} \end{bmatrix} = \begin{bmatrix} \langle \psi_{T,1} | H_{L-S} | \psi_{T,1} \rangle & \langle \psi_{T,1} | H_{L-S} | \psi_{T,0} \rangle & \langle \psi_{T,1} | H_{L-S} | \psi_{T,-1} \rangle & \langle \psi_{T,1} | H_{L-S} | \psi_{S,0} \rangle \\ \langle \psi_{T,0} | H_{L-S} | \psi_{T,1} \rangle & \langle \psi_{T,0} | H_{L-S} | \psi_{T,0} \rangle & \langle \psi_{T,0} | H_{L-S} | \psi_{T,-1} \rangle & \langle \psi_{T,0} | H_{L-S} | \psi_{S,0} \rangle \\ \langle \psi_{T,-1} | H_{L-S} | \psi_{T,1} \rangle & \langle \psi_{T,-1} | H_{L-S} | \psi_{T,0} \rangle & \langle \psi_{T,-1} | H_{L-S} | \psi_{T,-1} \rangle & \langle \psi_{T,-1} | H_{L-S} | \psi_{S,0} \rangle \\ \langle \psi_{S,0} | H_{L-S} | \psi_{T,1} \rangle & \langle \psi_{S,0} | H_{L-S} | \psi_{T,0} \rangle & \langle \psi_{S,0} | H_{L-S} | \psi_{T,-1} \rangle & \langle \psi_{S,0} | H_{L-S} | \psi_{S,0} \rangle \end{bmatrix}, \quad (11)$$

After that, we have:

$$|\psi_{T,m_s}\rangle = |R_{nl}\rangle |y_{lm}\rangle |\kappa_{T,m_s}\rangle, \quad (12)$$

$$|\psi_{S,0}\rangle = |R_{nl}\rangle |y_{lm}\rangle |\kappa_{S,0}\rangle. \quad (13)$$

We conclude that:

$$H_{L-S} = \frac{1}{\mu c^2} \langle R_{21} | \frac{1}{r} \frac{dV(r)}{dr} | R_{21} \rangle \times \begin{bmatrix} M_{11} & M_{12} & M_{13} & M_{14} \\ M_{21} & M_{22} & M_{23} & M_{24} \\ M_{31} & M_{32} & M_{33} & M_{34} \\ M_{41} & M_{42} & M_{43} & M_{44} \end{bmatrix}, \quad (14)$$

where M_{ij} is computed by the relations:

$$M_{11} = \langle y_{1,m} | \langle \kappa_{T,1} | \left[\frac{1}{2} (L_+ S_- + L_- S_+) + L_z S_z \right] | \kappa_{T,1} \rangle | y_{1,m} \rangle = \langle y_{1,m} | L_z | y_{1,m} \rangle \langle \kappa_{T,1} | S_z | \kappa_{T,1} \rangle = m \hbar^2, \quad (15)$$

$$M_{33} = \langle y_{1,m} | \langle \kappa_{T,-1} | \left[\frac{1}{2} (L_+ S_- + L_- S_+) + L_z S_z \right] | \kappa_{T,-1} \rangle | y_{1,m} \rangle = \langle y_{1,m} | L_z | y_{1,m} \rangle \langle \kappa_{T,-1} | S_z | \kappa_{T,-1} \rangle = -m \hbar^2, \quad (16)$$

where $m \in \{-1, 0, 1\}$. Other elements of M_{ij} in Equation (14) are equal to zero. It is important to point out here that each electron is spatially dependent on one atom of carbon and it is action just in spatial part. And since:

$$V(r) = -\frac{ze^2}{r}, \quad (17)$$

where z is the carbon atomic number. Thus, based on [17], the radial segment in Equation (14) is equal to:

$$\langle R_{21} | \frac{1}{r} \frac{dV(r)}{dr} | R_{21} \rangle = ze^2 \langle R_{21} | \frac{1}{r^3} | R_{21} \rangle = \frac{ze^2}{24a_0^3}, \quad (18)$$

where a_0 is the Boher radius. Based on Equations (15), (16) and (17), the Hamilton matrix turns into the following:

$$H_{L-S} = \begin{bmatrix} \frac{mze^2\hbar^2}{24\mu c^2 a_0^3} & 0 & 0 & 0 \\ 0 & 0 & 0 & 0 \\ 0 & 0 & \frac{-mze^2\hbar^2}{24\mu c^2 a_0^3} & 0 \\ 0 & 0 & 0 & 0 \end{bmatrix}. \quad (19)$$

To calculate the effect of fine structures through special value equation, the following determinant is used:

$$\begin{vmatrix} \frac{mze^2\hbar^2}{24\mu c^2 a_0^3} - \Delta E_{nL-S}^{(1)} & 0 & 0 & 0 \\ 0 & -\Delta E_{nL-S}^{(1)} & 0 & 0 \\ 0 & 0 & \frac{-mze^2\hbar^2}{24\mu c^2 a_0^3} - \Delta E_{nL-S}^{(1)} & 0 \\ 0 & 0 & 0 & -\Delta E_{nL-S}^{(1)} \end{vmatrix} = 0. \quad (20)$$

Based on various m , $m \in \{-1, 0, 1\}$, since the above determinant must be zero, we obtain:

$$\Delta E_{nL-S}^{(1)} \in \left\{ 0, \pm \frac{ze^2\hbar^2}{24\mu c^2 a_0^3} \right\}. \quad (21)$$

Hence, we have:

$$\Delta E_{n_{L-S}}^{(1)} \in \{0, \pm 1.45 \times 10^{-3}(\text{eV})\}. \quad (22)$$

Therefore, the difference in energy levels between singlet and triplet states, along with the alteration in the E_g value for the carbon-carbon bond, can be described as:

$$\Delta_0 = \Delta E_g = \Delta E_{L-S} = 2.9 \times 10^{-3} \text{eV}. \quad (23)$$

When a bond or several bonds are established among some carbon atoms, investigating the shift of gap energy would be more complex. This is even greater complexity in the case of carbon nanostructures that consist of several carbon bonds. Therefore, searching for methods and providing models is necessary for explicating changes in gap energy. In a single-ring carbon structure with N atoms, in which each atom is bonded solely with two other atoms, as shown in Figure 1, the mean of gap energy changes can be computed using the following formula:

$$\bar{\Delta}_1 = \left(\frac{b}{N}\right) \left(\frac{N_2}{b_2} \Delta_0\right) = \Delta_0, \quad (24)$$

where b is the number of bonds equal to N , N_2 and b_2 are the number of atoms which bond with individual carbon and the number of bonds between them respectively, and $N_2 = b_2 = 2$. But, in n ring structures, in which some atoms establish triple bonds, the mean of gap energy shifted is calculated in the following manner:

$$\bar{\Delta}_n = \left(\frac{b}{N}\right) [n\bar{\Delta}_1 + 3N_3\Delta_0], \quad (25)$$

where N_3 in the above formula is the number of atoms with triple bonds, and $b_3 = 1$ is the number of bonds between these atoms. Number 3 is the number of spin-orbit interactions between them.

In the family of linear acenes, we have (Figure 2):

$$N_3 = 2(n - 1), \quad (26)$$

$$b = 5n + 1, \quad (27)$$

$$N = 4n + 2. \quad (28)$$

According to Equations (24)-(28), gap energy changes in linear acene family are calculated as follows:

$$\bar{\Delta}_n = \left(\frac{5n + 1}{4n + 2}\right) (7n - 6) \Delta_0 \quad (\text{eV}). \quad (29)$$

The rest of the paper attempts to present a new model based on topological indices for gap energy changes in a linear acene family. Thus, RR , RM_2 , and RRR topological indices will be scrutinized in a linear acene family and the estimated values will be compared with those obtained from the quantum model, as shown in Equation (29).

Investigating gap energy changes becomes more difficult when the bond is established among several atoms of carbon. This becomes even more complex when the structure of multiple carbon atom bonds is on the nanoscale, which is why designing a model for calculating the changes in gap energy is so important. In continuation, we would like to calculate gap energy shifted in a linear acene family using topological indices.

3.2 RR , RM_2 , and RRR topological indices in linear acenes

At first, we compute RR , RM_2 , and RRR topological indices for a linear acene family. To establish a relation for each index based on the number of rings, these indices' values are then measured in some elements of linear acenes. Also, ΔE_g value is measured for the chosen members using the Hartree–Fock theory (HFT). Finally, we try to present an appropriate model to predict ΔE_g value in this family of elements, especially those with a large number of rings. According to Figure 1, we have the following theorem:

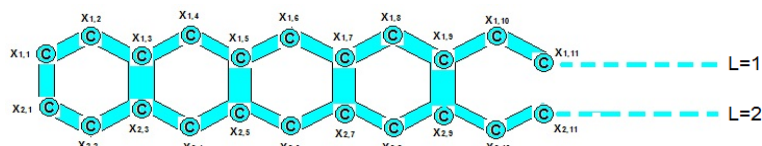


Figure 1: Simple molecular graph of linear acenes ($C_{4n+2}H_{2n+4}$).

Theorem 3.1. *If n represents the count of rings within a linear acene family, then the $RR(G)$ index can be expressed as:*

$$RR(G) = (3 + 4\sqrt{6})(n - 1) + 12. \quad (30)$$

Proof. Consider the simple graph in Figure 1, which can be divided into three regions:

- I. The set of all vertices and edges that are situated on or above the surface with a value of L equal to 1 is referred to as G_1 .

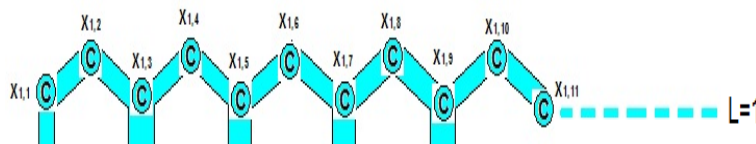


Figure 2: G_1 comprises of all vertices and edges positioned on or above the surface $L = 1$.

- II. The collection of vertices and edges that are positioned on surface $L = 2$ or above it is referred to as G_2 .

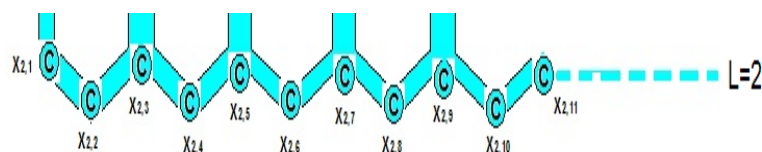


Figure 3: G_2 refers to all the vertices and edges that are positioned on surface $L = 2$ or below it.

- III. The collection of all vertices and edges lying in between the $L = 1$ and $L = 2$ surfaces is represented as G_3 .

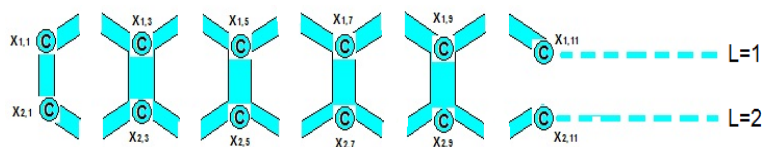


Figure 4: G_3 encompasses all the vertices and edges that lie within the surfaces defined by $L = 1$ and $L = 2$.

Based on Figure 2 and Equation (1), for G_1 we have:

$$RR(G_1) = \sum_{m=1}^{k-1} \sqrt{d_{1,m}d_{1,m+1}}, \quad (31)$$

where $d_{i,j}$ is degree of vertices $X_{i,j}$.

For the first and the last sentences in Equation (31), which are related to $X_{1,1}$ and $X_{1,k}$ vertices, we have:

$$\sqrt{d_{1,1}d_{1,2}} = \sqrt{d_{1,k-1}d_{1,k}} = 2. \quad (32)$$

And for $m \neq 1$ and $m \neq k - 1$, we have:

$$\sqrt{d_{1,m}d_{1,m+1}} = \sqrt{6}. \quad (33)$$

Therefore, based on Equations (32) and (33), Equation (31) is obtained as follows:

$$RR(G_1) = 2 + \sum_{m=2}^{k-2} \sqrt{6} + 2. \quad (34)$$

And since $k = 2n + 1$,

$$RR(G_1) = 4 + \sqrt{6} [(k - 2) - 1] = 4 + 2\sqrt{6} (n - 1). \quad (35)$$

The same conclusion is applicable to G_2 as shown in Figure 3:

$$RR(G_2) = 4 + 2\sqrt{6}(n - 1). \quad (36)$$

However, for G_3 , based on Figure 4, and since in $X_{1,m}$ all of m values are odd numbers, we have:

$$RR(G_3) = \sqrt{d_{1,1}d_{2,1}} + \sqrt{d_{1,k}d_{2,k}} + \sum_{m=2}^{\frac{k-1}{2}} \sqrt{d_{1,m}d_{2,m}}. \quad (37)$$

Since:

$$\sqrt{d_{1,1}d_{2,1}} = \sqrt{d_{1,k}d_{2,k}} = 2, \quad (38)$$

we have:

$$RR(G_3) = 4 + 3\left[\left(\frac{k-1}{2}\right) - 1\right] = 4 + 3(n - 1). \quad (39)$$

And since:

$$RR(G) = RR(G_1) + RR(G_2) + RR(G_3), \quad (40)$$

based on Equations (35), (36), (39), and (4), the proof is completed. ■

Theorem 3.2. *If n represents the number of rings present in linear acenes, the value of the $RM_2(G)$ index can be expressed as follows:*

$$RM_2(G) = 12n - 6. \quad (41)$$

Proof. Assume that the simple graph in Figure 1 can be applied to three regions of G_1, G_2 , and G_3 as shown in Figures 2 to 4. In this case, the RM_2 index with Equation (2) for G_1 is as follows:

$$RM_2(G_1) = \sum_{m=1}^{k-1} (d_{1,m} - 1)(d_{1,m+1} - 1). \quad (42)$$

Since

$$(d_{1,1} - 1)(d_{1,2} - 1) = (d_{1,k-1} - 1)(d_{1,k} - 1) = 1. \quad (43)$$

For $m \neq 1, k - 1$:

$$(d_{1,m} - 1)(d_{1,m+1} - 1) = 2. \quad (44)$$

We have:

$$RM_2(G_1) = 1 + 1 + \sum_{m=2}^{k-2} 2 = 2 + 2[(k - 2) - 1]. \quad (45)$$

Since $k = 2n + 1$, we have

$$RM_2(G_1) = 2 + 4(n - 1). \quad (46)$$

The same conclusion is applicable to the G_2 region shown in Figure 3.

$$RM_2(G_2) = RM_2(G_1) = 2 + 4(n - 1). \quad (47)$$

But for the G_3 region, based on Figure 4, and since m in the $X_{1,m}$ equation includes odd numbers, by separating the first and the last vertices, we get:

$$RM_2(G_3) = (d_{1,1} - 1)(d_{2,1} - 1) + (d_{1,k} - 1)(d_{2,k} - 1) + \sum_{m=2}^{\frac{k-1}{2}} (d_{1,m} - 1)(d_{2,m} - 1). \quad (48)$$

Then, we obtain:

$$RM_2(G_3) = 1 + 1 + 4\left[\left(\frac{k-1}{2}\right) - 1\right] = 2 + 4(n - 1). \quad (49)$$

Therefore, the proof of theorem is completed by Equations (46), (47), and (49).

$$RM_2(G) = RM_2(G_1) + RM_2(G_2) + RM_2(G_3) = 12n - 6. \quad (50)$$

■

Theorem 3.3. *Let's denote the total number of rings in linear acenes as n . In this context, the $RRR(G)$ index can be defined as follows:*

$$RRR(G) = 6 + (n - 1)[2 + 4\sqrt{2}]. \quad (51)$$

Proof. Assume that simple graph in Figure 1 can be applied to three regions. Based on Figure 2 and Equation (3), for G_1 area we will have:

$$RRR(G_1) = \sum_{m=1}^{k-1} \sqrt{(d_{1,m} - 1)(d_{1,m+1} - 1)}. \quad (52)$$

For the first and the last sentence in Equation (52), which is related to $X_{1,1}$ and $X_{1,k}$ vertices:

$$\sqrt{(d_{1,1} - 1)(d_{1,2} - 1)} = \sqrt{(d_{1,k-1} - 1)(d_{1,k} - 1)} = 1, \quad (53)$$

and for $m \neq 1, k - 1$, we have:

$$\sqrt{(d_{1,m} - 1)(d_{1,m+1} - 1)} = \sqrt{2}. \quad (54)$$

Therefore, by using Equations (53) and (54), we have:

$$RRR(G_1) = 1 + \sum_{m=2}^{k-2} \sqrt{2} + 1. \quad (55)$$

And since $k = 2n + 1$, we have:

$$RRR(G_1) = 2 + \sqrt{2}[(k - 2) - 1] = 2 + 2\sqrt{2}(n - 1). \quad (56)$$

The same conclusion applies to the G_2 region, as shown in Figure 3.

$$RRR(G_2) = 2 + (n - 1). \quad (57)$$

But for G_3 , based on Figure 4, and since m in $X_{1,m}$ equation includes odd numbers, we have:

$$RRR(G_3) = \sqrt{(d_{1,1} - 1)(d_{2,1} - 1)} + \sqrt{(d_{1,k} - 1)(d_{2,k} - 1)} + \sum_{m=2}^{\frac{k-1}{2}} \sqrt{(d_{1,m} - 1)(d_{2,m} - 1)}. \quad (58)$$

Since

$$\sqrt{(d_{1,1} - 1)(d_{2,1} - 1)} = \sqrt{(d_{1,k} - 1)(d_{2,k} - 1)} = 1, \quad (59)$$

and

$$\sqrt{(d_{1,m} - 1)(d_{2,m} - 1)} = 2, \quad (60)$$

we have

$$RRR(G_3) = 4 + 2\left[\left(\frac{k-1}{2}\right) - 1\right] = 2 + 2(n - 1), \quad (61)$$

and since we have

$$RRR(G) = RRR(G_1) + RRR(G_2) + RRR(G_3). \quad (62)$$

Therefore, the proof is completed. ■

Table 1: $RR(G)$, $RRR(G)$, and $RM_2(G)$ indices and value in linear acenes using HF and quantum perturbations theory.

n - acene	RR Index	RRR index	RM_2 index	ΔE_g (eV)- HF	Δ (eV)
1- acene	12	6	6	0.00392	0.0029
2- acene	24.7979	13.6568	18	0.01625	0.02552
3- acene	37.5958	21.3136	30	0.03649	0.0497
4- acene	50.3937	28.9704	42	0.06129	0.0744
5- acene	63.1916	36.6272	54	0.08887	0.0993
6- acene	75.9895	44.1952	66	0.11823	0.1244
7- acene	88.7874	51.852	78	0.14854	0.1496
8- acene	101.5853	59.5088	90	0.17954	0.1748

4 Results and discussion

To obtain a model based on topological indices, nine elements of linear acenes are chosen and computed. The topological indices are $RR(G)$, $RRR(G)$, and $RM_2(G)$, the results of which are shown in Table 1. The last two columns of Table 1 show the calculated values of the elected members of the linear acene family. These have been obtained using the HF method [25] and the model developed by Equation (29).

Figure 5 shows gap energy changes in linear acenes based on $RM_2(G)$. As it shows, this index predicts gap energy changes with high precision of ($R^2 = 0.9989$).

$$\Delta E_g = 8 \times 10^{-6}(RM_2)^2 + 13 \times 10^{-4}(RM_2) - 81 \times 10^{-4}(\text{eV}). \quad (63)$$

The following equation ΔE_g is obtained according to Figure 5:

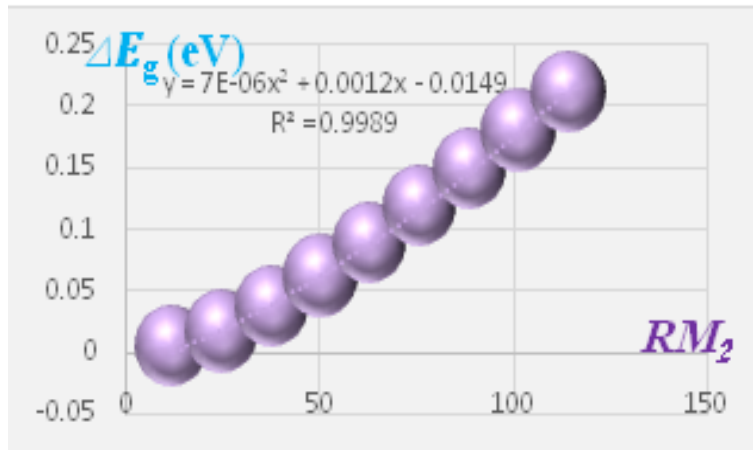
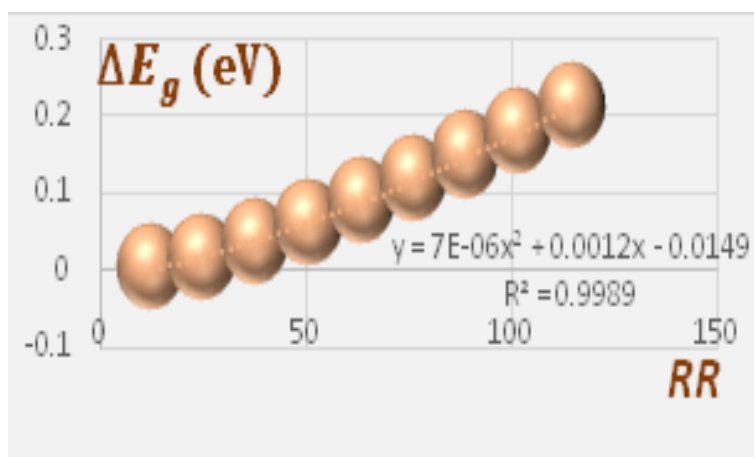
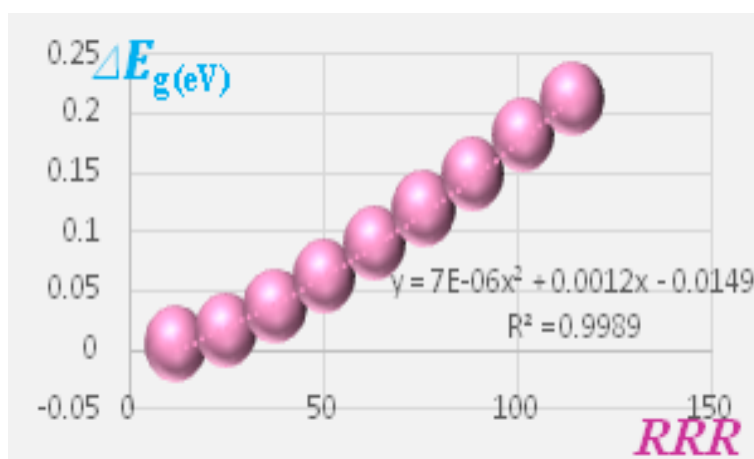


Figure 5: Gap energy changes based on $RM_2(G)$ in linear acenes.

Gap energy changes for linear acenes were calculated based on $RR(G)$ and $RRR(G)$ indices, and the results are shown in Figures 6 and 7.

Figures 6 and 7 indicate the success and precision ($R^2 = 0.9989$ and $R^2 = 0.9988$) of these indices in predicting gap energy changes in linear acenes, as shown in the following equations:

$$\Delta E_g = 7 \times 10^{-6}(RR)^2 + 1.2 \times 10^{-3}(RR) - 1.49 \times 10^{-2}(\text{eV}), \quad (64)$$

Figure 6: Gap energy changes based on $RR(G)$ in linear acenes.Figure 7: Gap energy shifted based on $RRR(G)$ in linear acenes.

$$\Delta E_g = 2 \times 10^{-5}(RRR)^2 + 2.2 \times 10^{-3}(RRR) - 1.46 \times 10^{-2}(\text{eV}). \quad (65)$$

5 Conclusion

Gap energy shifted is computed using quantum perturbation theory and the HF method. Furthermore, this article introduces three models that rely on topological indices to explain variations in the gap energy of acenes. These models are made for gap energy changes in this group of elements based on three indices— RM_2 , RR , and RRR —which are denoted with Equations (63), (64), and (65). In more complex acenes, as the number of carbon atoms increases, so does the number of levels in the conduction and valence bonds. Consequently, the highest occupied molecular orbital (HOMO) moves upwards, while the lowest unoccupied molecular orbital (LUMO) moves downwards. Simultaneously, there is an increase in the electron cloud. This means reduced energy gap by increasing the number of loops, so this is quite logical that the gap energy changes were increased.

Although these three models provide high accuracy of computational methods, the model is most successful when based on the RM_2 index.

Author Contributions. B.A.K. conceived of the presented idea. A.I. developed the theory, performed the computations and verified the analytical methods.

Conflicts of interest. The authors declare that they have no conflicts of interest regarding the publication of this article.

References

- [1] A. J. Pérez-Jiménez and J. C. Sancho-Garcia, Conductance enhancement in nanographene-gold junctions by molecular π -stacking, *J. Am. Chem. Soc.* **131** (2009) 14857–14867, <https://doi.org/10.1021/ja904372d>.
- [2] J. C. Sancho-Garcia and A. J. Pérez-Jiménez, Charge-transport properties of prototype molecular materials for organic electronics based on graphene nanoribbons, *Phys. Chem. Chem. Phys.* **11** (2009) 2741–2746, <https://doi.org/10.1039/B821748C>.
- [3] D. Jiang and S. Dai, Circumacenes versus periacenes: HOMO-LUMO gap and transition from nonmagnetic to magnetic ground state with size, *Chem. Phys. Lett.* **466** (2008) 72–75, <https://doi.org/10.1016/j.cplett.2008.10.022>.
- [4] F. Koorepazan-Moftakhar, A. R. Ashrafi, O. Ori and M. V. Putz, *Sphericity of Some Classes of Fullerenes Measured by Topology, Chapter 11, Fullerenes: Chemistry, Natural Sources and Technological Applications*, Nova Science Publishers, 2014, 285–304.
- [5] D. Bonchev, O. Mekenyan and V. Kamenska, A topological approach to the modeling of polymer properties, *J. Math. Chem.* **11** (1992) 107–132, <https://doi.org/10.1007/BF01164197>.
- [6] D. J. Klein and D. Babić, Partial orderings in chemistry, *J. Chem. Inf. Comput. Sci.* **37** (1997) 656–671, <https://doi.org/10.1021/ci9601776>.
- [7] I. Gutman, B. Furtula and C. Elphick, Three, new/old vertex–degree–based topological indices, *MATCH Commun. Math. Comput. Chem.* **72** (2014) 617–632.
- [8] A. T. Balaban, *Chemical Applications of Graph Theory*, Academic Press, London, UK, 1976.
- [9] J. Devillers and A. T. Balaban, (Eds.), *Topological Indices and Related Descriptors in QSAR and QSPR*, Gordon and Breach, Amsterdam, The Netherlands, 1999.
- [10] R. Garcia-Domenech, A. Villanueva, J. Galvez and R. Gozalbes, Application de la topologie moleculaire a la prediction de la viscosite liquide des composes organiques, *J. Chim. Phys.* **96** (1999) 1172–1185, <https://doi.org/10.1051/jcp:1999205>.
- [11] O. Ivanciuc, T. Ivanciuc and A. T. Balaban, Quantitative structure-property relationship study of normal boiling points for halogen-/ oxygen-/ sulfur-containing organic compounds using the CODESSA program, *Tetrahedron* **54** (1998) 9129–9142, [https://doi.org/10.1016/S0040-4020\(98\)00550-X](https://doi.org/10.1016/S0040-4020(98)00550-X).

- [12] K. C. Das and I. Gutman, Some properties of the second Zagreb index, *MATCH Commun. Math. Comput. Chem.* **52** (2004) 103–112.
- [13] A. Iranmanesh and Y. Pakraves, Edge detour index of TUC4C8(S) nanotube, *Optoelectron. Adv. Mater. Rapid Commun.* **4** (2010) 264–266.
- [14] M. Azari and A. Iranmanesh, Harary index of some nano-structures, *MATCH Commun. Math. Comput. Chem.* **71** (2014) 373–382.
- [15] M. Azari and A. Iranmanesh, Chemical graphs constructed from rooted product and their Zagreb indices, *MATCH Commun. Math. Comput. Chem.* **70** (2013) 901–919.
- [16] A. Iranmanesh and M. V. Diudea, Cluj-Tehran index, *MATCH Commun. Math. Comput. Chem.* **69** (2013) 121–130.
- [17] A. Iranmanesh and Y. Alizadeh, Balaban and Randic indices of IPRC80 fullerene Isomers, Zigzag nanotubes and grapheme, *Int. J. Nanosci. Nanotechnol.* **7** (2011) 28–34.
- [18] A. Iranmanesh and Y. Alizadeh, Computing Wiener and Schultz indices of HAC5C7 [p, q] nanotube by GAP program, *Am. J. Appl. Sci.* **5** (2008) 1754–1757, <https://doi.org/10.3844/ajassp.2008.1754.1757>.
- [19] R. Kazemi, A. Behtoei and A. Kohansal, The Zagreb index of bucket recursive trees, *Math. Interdisc. Res.* **5** (2020) 103–111, <https://doi.org/10.22052/MIR.2020.204312.1166>.
- [20] A. Ebrahimi, M. Monemzadeh, H. Moshafi and SMS Movahed, Tension reduction between planck data and LSS by dynamical dark energy model, *Math. Interdisc. Res.* **5** (2020) 113–130, <https://doi.org/10.22052/MIR.2019.176929.1127>.
- [21] M. Azari, On eccentricity version of Zagreb coindices, *Math. Interdisc. Res.* **6** (2021) 107–120, <https://doi.org/10.22052/MIR.2021.240325.1247>.
- [22] F. Movahedi, Bounds on the minimum edge dominating energy in terms of some parameters of a graph, *Math. Interdisc. Res.* **8** (2023) 175–187, <https://doi.org/10.22052/MIR.2023.248452.1379>.
- [23] J. J. Sakurai, *Advanced Quantum Mechanics*, Addison-Wesley, 1967.
- [24] D. J. Griffiths, *Introduction to Quantum Mechanics, 2nd Edition*, Addison-Wesley Press, Boston, 2004.
- [25] E. San-Fabián and F. Moscardó, Polarized–unpolarized ground state of small polycyclic aromatic hydrocarbons, *Int. J. Quantum Chem.* **113** (2013) 815–819, <https://doi.org/10.1002/qua.24090>.